



Article

# Systematic Study of Vibrational Spectra of Octahedral Rhenium Clusters $\{Re_6S_{8-x}Br_x\}Br_y$ (x = 0, 1, 2, 3, 4) with Mixed Sulfur/Bromine Inner Ligands

Alexandra Yu. Ledneva \*, Mariia N. Ivanova, Pavel A. Poltarak, Spartak S. Yarovoy, Boris A. Kolesov, Vladimir E. Fedorov and Nikolay G. Naumov

Nikolaev Institute of Inorganic Chemistry, Siberian Branch of Russian Academy of Sciences, 630090 Novosibirsk, Russia

\* Correspondence: ledneva@niic.nsc.ru

**Abstract:** A series of rhenium compounds with the octahedral cluster core  $\{Re_6S_{8-x}Br_x\}$  (x=0-4): with molecular and polymeric structure were obtained. In these compounds the cluster core composition varies monotonically, the geometry of the cluster and the rhenium coordination polyhedron are retained unchanged, while the symmetry of the cluster changes. The vibrational spectra (Raman and IR) were recorded and analyzed for compounds with all possible S/Br ratios in the cluster core. The group vibrations of clusters were attributed with the use of DFT calculations of vibrational spectra. It is shown that the set of main characteristic bands is retained in both ionic and polymeric compounds regardless of the composition and the symmetry of the cluster core while the observed vibration frequencies of these bands depend on the S/Br ratio in the cluster core. In particular, the group Re–S stretching vibrations ( $A_{1g}(S_8)$  and  $T_{2g}(S_8)$  modes) shifted to higher frequencies with the increase in the number of Br atoms in the cluster. The difference in the connectivity in polymeric compounds leads to an increase in the number of bands in the spectra and to the disappearance of the  $A_{1g}(Br)$  modes.

Keywords: rhenium cluster; Raman spectra; IR spectra; DFT



Citation: Ledneva, A.Y.; Ivanova, M.N.; Poltarak, P.A.; Yarovoy, S.S.; Kolesov, B.A.; Fedorov, V.E.; Naumov, N.G. Systematic Study of Vibrational Spectra of Octahedral Rhenium Clusters {Re<sub>6</sub>S<sub>8-x</sub>Br<sub>x</sub>}Br<sub>y</sub> (x = 0, 1, 2, 3, 4) with Mixed Sulfur/Bromine Inner Ligands. *Symmetry* **2023**, *15*, 1791. https://doi.org/10.3390/sym15091791

Academic Editor: Franc Perdih

Received: 30 August 2023 Revised: 14 September 2023 Accepted: 18 September 2023 Published: 19 September 2023



Copyright: © 2023 by the authors. Licensee MDPI, Basel, Switzerland. This article is an open access article distributed under the terms and conditions of the Creative Commons Attribution (CC BY) license (https://creativecommons.org/licenses/by/4.0/).

# 1. Introduction

Rhenium octahedral chalcogenide and chalcohalide cluster complexes are the typical examples of transition metal high-valence clusters [1–5]. The structures of such clusters are based on the Re<sub>6</sub> octahedron, each face of which is co-ordinated by  $\mu_3$ -bridging inner ligands, forming the  $\{Re_6Q_8\}^n$  or  $\{Re_6Q_{8-x}Y_x\}^n$  cluster core (Q = S, Se, Te, Y = Cl, Br, I,x = 1-4). Each rhenium is additionally coordinated by apical ligand L, forming the general formula of  $\{Re_6Q_8\}L_6$  or  $\{Re_6Q_{8-x}Y_x\}L_6$  for a discrete cluster fragment. Compounds based on Re<sub>6</sub> clusters are attractive due to promising structural features and physicochemical properties of compounds based on them. Among the latter, one can consider intense red luminescence [4,6–9], electronic and magnetic properties [10–16], and highly effective X-ray contrast properties [17–19]. Well-developed apical ligand exchange chemistry along with chemical stability and rigid geometry of the cluster core allows the designing of unique hybrid materials, e.g., liquid crystal phases [20-23], polymeric matrixes with immobilized clusters [20,24,25], and cluster-coated surfaces [26,27]. Discrete  $\{Re_6Q_{8-x}Y_x\}L_6$  structural units were found to be promising building blocks for the bottom-up design of different types of supramolecular arrays, e.g., coordination polymers and extended molecular solids [28-37].

To date, the main methods for structural study of such compounds are diffraction methods: X-ray structural analysis and powder diffraction. These methods are well suited for crystalline phases with long-range order, and, to a lesser extent, for hybrid materials, e.g., liquid crystal phases, nanoparticles, and cluster-coated surfaces.

Symmetry 2023, 15, 1791 2 of 12

Vibrational spectroscopy (Raman and IR) is a powerful and widely used method for structural characterization of crystalline and non-crystalline phases, but its application to octahedral chalcogenide and chalcohalide rhenium clusters is very limited. Probably, the only example of a systematic study of Raman spectra of complexes  $[\{Re_6Q_8\}Y_6]^{4-}$  (Q = S, Se; Y = Cl, Br, I) in comparison with spectra calculated by the DFT method is the work of Gray et al. [6].

In the present work, we systematically study by experimental and DFT methods the vibrational spectra (Raman and IR) of a family of compounds based on  $\{Re_6S_{8-x}Br_x\}\{x=0,1,2,3,4\}$  core: salts of ionic/molecular complexes  $[\{Re_6S_{8-x}Br_x\}Br_6]^{4-x}$  and ternary phases  $[\{Re_6S_{8-x}Br_x\}Br^2\}Br^2]^{4-x}$ . Evidently, the clusters are the large polyatomic moieties in which all vibrations have a group nature with a significant contribution of a large number of atoms to each vibration mode, therefore, the analysis is complicated and requires the support of quantum calculations. In compounds with the  $\{Re_6S_8\}^{2+}$  cluster core, the  $Re_6$  octahedron is coordinated by eight inner  $\mu_3$ - $S^i$  ligands arranged along the eight vertices of the cube. In compounds with the  $[\{Re_6S_{8-x}Br_x\}]$  cluster core, both  $S^i$  and  $Br^i$ , which are always disordered in crystal structure, are located in the inner sphere, such that the geometry and the number of ligands around the metal cluster  $Re_6$  remain the same. The number of cluster skeletal electrons is also constant, which simplifies comparative analysis of the data.

Thus, two series of octahedral Re(III) clusters—anionic complexes and ternary thiobromides in which the metal atoms have the same coordination polyhedron but a monotonically changing environment in the plane of the rhenium atom—are good model objects for study by vibrational spectroscopy, accompanied by DFT calculations.

### 2. Materials and Methods

X-ray powder diffraction (XRPD) patterns were collected with a Philips PW 1830/1710 automated diffractometer (Cu K $\alpha$  radiation, graphite monochromator, silicon plate as an external standard, 20 5–60°, step 0.05, 2 s), before recording samples were ground in a mortar in hexane. Far infra-red spectra of samples in a polyethylene tablet were recorded with a FTIR spectrometer VERTEX 80. Raman spectra were recorded with a Raman spectrometer LabRAM HR Evolution, with excitation by the 632 and 514 nm lines of He-Ne and Ar<sup>+</sup> lasers, and single crystals or polycrystalline samples were collected for analysis. If the luminescence of the sample hindered the analysis of the Raman spectrum, the background level was extrapolated by the second polynomial and subtracted from the experimental spectrum. Energy-dispersive spectroscopy was performed with a Hitachi TM3000 device.

Optimization of the geometric parameters of molecules and anions of the composition  $[Re_6S_{8-x}Br_xBr_6]^{(4-x)-}$  were performed using the density functional theory in the software package AMS2022 [38]. The calculations were conducted according to the TZP all-electronic basis [39] using a GGA BP86 functional [40]. The zero-order regular approximation (ZORA) was used in all calculations in this work to take into account the scalar relativistic effects [41].

All Re $_6$  cluster compounds were obtained by high-temperature synthesis from elements in evacuated quartz ampoules under the same conditions (750 °C, 72 h), except for Re $_6$ S $_8$ Br $_2$  prepared at 1100 °C. Ionic compounds were obtained from stoichiometric amounts of MBr (M = K or Cs), Re, S, and Br $_2$  (with 5% excess) [42–45]. Resulting powders were dissolved in water with the addition of HBr, and insoluble precipitates were filtered and removed. Dark red solutions were evaporated; red crystal powders were collected and dried with air. Polymeric compounds were synthesized from stoichiometric amounts of Re, S, and Br $_2$  (with 5% excess) [46–49]. Products were washed with acetone and dried with air. The purity of the obtained compounds was confirmed by powder diffraction and elemental analysis data.

Symmetry **2023**, *15*, 1791 3 of 12

#### 3. Results and Discussion

Vibrational (Raman or IR) spectra contain almost all structural information about the compound, but the use of these methods in investigation of octahedral Re<sub>6</sub> cluster complexes is very limited. This is due to several reasons that hinder their usage for characterizing, e.g., the complexity of the spectrum, a large number of spectral lines in a narrow spectral range, and, as a result, low characteristic vibrations. In the case when a complete interpretation of the spectra is impossible, it is quite sufficient to follow the characteristic modes to draw conclusions about the preservation of the structure during the process [16,27]. Two approaches are used to interpret the spectra: vibrations in clusters refer to individual bond fluctuations, or to collective vibrations of the cluster as a whole. The second approach is certainly correct, since all vibrations in the spectrum are mixed and include displacements of all atoms of the molecule, but the relative lightness (i.e., small mass) of ligand atoms compared to the mass of metal atoms sometimes allows us to consider their vibrations as individual ones.

Both in anionic complexes  $[Re_6S_{8-x}Br_x]Br_6^{(4-x)-}$  (x=0-4) and in ternary thiobromides  $[Re_6S_{4+x}Br_{10-2x}]$  (x=0,1,3,4), the coordination polyhedron of rhenium atoms is the same, but the Br/S ratio in the cluster core from  $\{Re_6S_8\}$  to  $\{Re_6S_4Br_4\}$  changes. For all cases, the coordination environment of each rhenium atom lying in the  $\mu_3$  ligand plane can be written as follows:  $Re_4(S/Br)_4{}^iBr^a$  (i—inner, a—apical, according to the Schäfer notation [50]). An exception is  $Re_6S_8Br_2$ , in which some of the sulfide ligands are simultaneously inner  $S^i$  for one  $Re_6$  metal cluster and apical  $S^a$  for the neighboring one. This becomes clearer if we write down the structural formula of  $Re_6S_8Br_2$  as  $[\{Re_6S_6^ic_{5^{i-a}2/2}\}S_{2/2}^{a-i}Br_{5^{a-a}4/2}]$  [49].

To avoid the excess of formulas in the text of the article, we introduced the following designations for the studied compounds:  $\mathbf{np}$ ,  $\mathbf{ni}$ , and  $\mathbf{nm}$ , where the number n indicates the number of sulfur atoms in the cluster core {Re<sub>6</sub>S<sub>8-x</sub>Br<sub>x</sub>}, (x = 0–4) and the letter the type of compound:  $\mathbf{p}$ —polymeric,  $\mathbf{i}$ —anionic complex, and  $\mathbf{m}$ —neutral molecular complex Re<sub>6</sub>S<sub>4</sub>Br<sub>10</sub>. The composition, structure, and possible isomers of thus designated compounds are presented in Table 1.

Table 1. List of investigated compounds, its isomers and designations in text.

Polymer Structure	Ionic Structure	Isomers (Inner S/Br Positions)
		x = 8
$\begin{array}{l} Re_6S_8Br_2 \ \textbf{(8p)} \\ [\{Re_6S^i_6S^{i-a}_{2/2}\}S_{2/2}{}^{a-i}Br^{a-a}_{4/2}] \ ^* \\ 3D \ polymer \end{array}$	$Cs_4Re_6S_8Br_6$ (8i) $Cs_4\{Re_6S^i_{\ 8}\}Br^a_{\ 6}$	Oh Re Br S
		x = 7
Re <sub>6</sub> S <sub>7</sub> Br <sub>4</sub> <b>(7p)</b> {Re <sub>6</sub> S <sup>i</sup> <sub>7</sub> Br <sup>i</sup> }Br <sup>a</sup> <sub>6/2</sub> 3D polymer	Cs <sub>3</sub> Re <sub>6</sub> S <sub>7</sub> Br <sub>7</sub> <b>(7i)</b> Cs <sub>3</sub> {Re <sub>6</sub> S <sub>7</sub> <sup>i</sup> Br <sup>i</sup> }Br <sup>a</sup> <sub>6</sub>	Cav

Symmetry **2023**, 15, 1791 4 of 12

Table 1. Cont.

Ionic Structure	Isomers (Inner S/Br Positions)
	x = 6
$\begin{aligned} &M_{2}Re_{6}S_{6}Br_{8}\ (M=Cs\ or\ K)\ \textbf{(6i)}\\ &M_{2}\{Re_{6}S^{i}{}_{6}Br^{i}{}_{2}\}Br^{a}{}_{6}\end{aligned}$	C <sub>2v</sub> C <sub>2v</sub> D <sub>3d</sub>
	x = 5
KRe <sub>6</sub> S <sub>5</sub> Br <sub>9</sub> <b>(5i)</b> K{Re <sub>6</sub> S <sup>i</sup> <sub>5</sub> Br <sup>i</sup> <sub>3</sub> }Br <sup>a</sup> <sub>6</sub>	C <sub>s</sub> C <sub>3ν</sub> C <sub>s</sub> 2 3
	x = 4
	$M_2Re_6S_6Br_8 \ (M = Cs \ or \ K) \ (6i)$ $M_2\{Re_6S_6^iBr_2^i\}Br_6^a$ $KRe_6S_5Br_9 \ (5i)$

<sup>\*</sup> Chemical formula according to Schäfer notation [50]; i—inner, a—apical.

### 3.1. Raman Spectroscopy

Raman spectra of cluster compounds of the presented series were obtained both experimentally (for all compounds) and via DFT calculations (for ionic and molecular compounds). The unsubstituted 8i cluster has no geometric isomers (as for 7i, there is only one form) and its spectrum is described in detail [6]. Replacement of sulfur atoms by bromine in the cluster core leads to the appearance of isomeric forms for 6i, 5i, and 4m, for which it is possible to calculate the spectra separately. Moreover, replacement leads to changing of the charge and the symmetry of the cluster, which, in turns, leads to changing of the spectrum profile (see Figures 1 and S1–S4). Considering the calculated spectra, three main regions of vibrations can be distinguished: 380–460, 120–200, and 55–95 cm<sup>-1</sup>. These three regions are marked in the experimentally obtained spectra of ionic 8i-5i and molecular 4m complexes in Figure 1 as I, II, and III, respectively. The first are vibrations in the 380-460 cm<sup>-1</sup> region (region I in Figure 1), which in cluster 8i are attributed to vibrations A<sub>1g</sub>(S<sub>8</sub>) and T<sub>2g</sub>, i.e., in fact, to group Re–S stretching vibrations [6]. Moreover, the band in the region of  $\sim$ 420 cm<sup>-1</sup> refers to the symmetric vibration A<sub>1g</sub>, i.e., all bonds simultaneously either lengthen or shorten, and the band at about 390 cm<sup>-1</sup> is asymmetric; some of the bonds lengthen while the rest shorten. The region  ${\bf II}$  around 150 cm $^{-1}$  can be attributed to symmetric vibrations  $A_{1g}(Br^a)$  ( $\nu(Re-Br^a)$ ), and in the region III of 60 cm<sup>-1</sup>  $\delta$ 

Symmetry **2023**, 15, 1791 5 of 12

or  $\rho(Br)$  (bromine atoms "rock" relative to the cluster, i.e., the angle Br-Re- $\mu_3L$  changes). When analyzing calculated Raman spectra of clusters 8i-5i and 4m in these regions several oscillations with a similar type are observed. Note that experimental samples contain clusters with a different symmetry type (see Table 1), and even mixtures of isomers with different symmetry. Therefore, the theoretical description of each vibrational mode is rather complicated. However, the profiles look similar, and, for easier understanding, we utilize the same symbols as the parent spectrum for 8i.

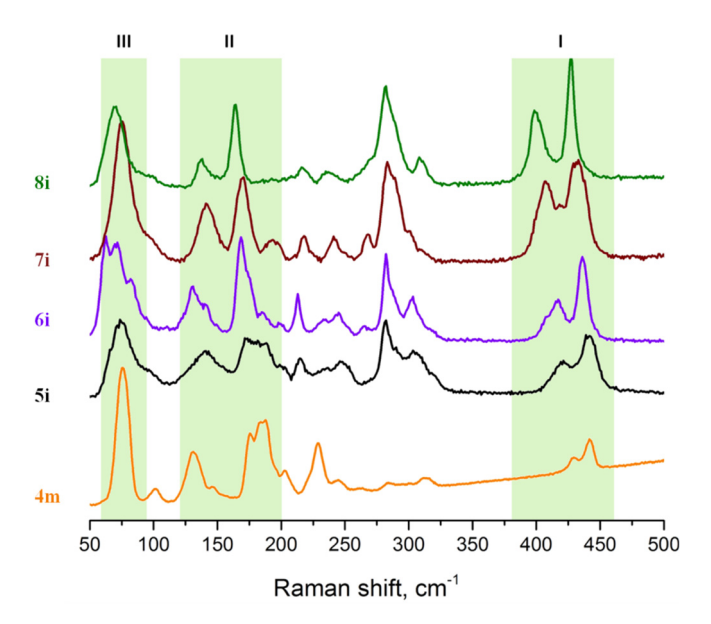


**Figure 1.** Raman spectra of ionic **5i–8i** in comparison with molecular **4m** cluster. Green rectangles indicate regions under detailed consideration, i.e., 380–460, 120–200, and 55–95 cm<sup>-1</sup> marked **I**, **II**, and **III**, respectively.

Modes in the remaining regions can be attributed to the complex type, i.e., almost all atoms in the cluster complex are shifting from their initial positions. For example, "breathing" cluster vibration, also attributed to  $A_{1g}(Re_6)$ , located at 275 cm<sup>-1</sup> for 8i, also involve sulfur atoms to a lesser extent. Despite the fact that the replacement of inner sulfur atoms by bromine actually changes the geometry and lowers the symmetry of the cluster, the oscillations observed in the regions about 420 and 150 cm<sup>-1</sup> are referred to as " $A_{1g}$ " in the work, as they resemble the motif of the corresponding ones for 8i. It should be noted that in the region of 100–320 cm<sup>-1</sup>, the spectra become more complicated and many additional bands appear. Furthermore, the appearance of isomeric forms for cluster complexes 6i, 5i, and 4m complicates the experimental spectrum, that being a superposition of spectra of isomers (Figures S2–S4). Despite the calculated ratio of isomeric forms, for example, for 5i as 3:3:1, the real ratio may reach other values [51,52], making the interpretation of the experimental spectra more difficult.

Experimental Raman spectra for 8i–5i and 4m (Figure 1) were compared with the corresponding calculated spectra (Figures S1–S4). In the case of unsubstituted 8i cluster, there are only two intense bands in the region of 380–460 cm $^{-1}$ , i.e.,  $A_{1g}(S_8)$  and  $T_{2g}(S_8)$  oscillations (region I, Figure 2). The vibration at 428 cm $^{-1}$  for 8i is the fully symmetrical vibration  $A_{1g}(S)$ . Displacement of atoms in the 8i cluster during  $A_{1g}(S_8)$  vibrations is shown schematically in Figure 2b. When comparing the spectra in the series of ionic compounds 5i–8i and molecular 4m, it can be seen that increasing the number of Br atoms in the cluster core leads to a shift of the peak towards higher frequencies, up to 442 cm $^{-1}$  for 4m (Figure 2c). This is probably due to the sum of force constants, which for the metal remains approximately unchanged regardless of the number of ligands or their types. This total value represents a certain ability of the metal to use all its valence electrons to bond with the environmental atoms. For this reason, if sulfur is replaced by bromine the

Symmetry **2023**, 15, 1791 6 of 12

bonding with rhenium is changed. The character of this change could be explained by the effect of electronegativity. When Br as a more electronegative atom than S is introduced in the cluster core  $\{Re_6S_8\}$ , the bond Re–S becomes more covalent, and the force constant increases. Another noticeable mode in the region I is the  $T_{2g}(S_8)$  fluctuation at  $400~\text{cm}^{-1}$  for 8i. When sulfur is replaced by bromine, this band is broadened in the spectra and additional bands of low intensity appear which is caused by a change in the symmetry of the cluster and the nonequivalence of sulfur atoms. However, despite this, the position of the main most intense  $A_{1g}(S)$  and  $T_{2g}(S)$  bands changes linearly when sulfur is replaced by bromine (Figure 2c).

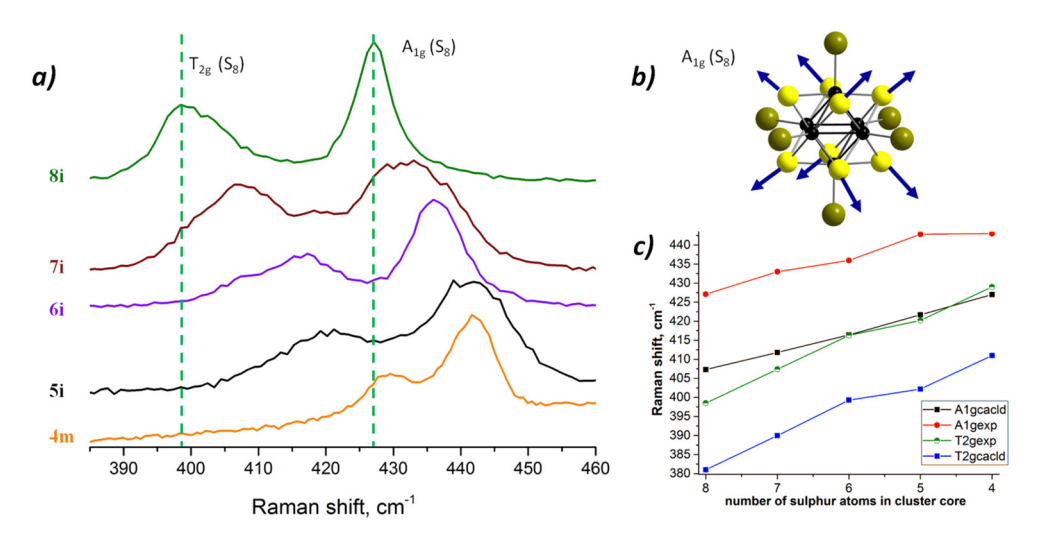


**Figure 2.** Comparison of Raman spectra **4m** with ionic **5i–8i** in the region I (**a**). Vertical dotted lines are drawn from the **8i** peaks. The oscillation  $A_{1g}(S_8)$  is shown schematically on (**b**). Dependence of the  $A_{1g}$  and  $T_{2g}$  band position on the degree of substitution (calculation and experiment) (**c**).

The spectra of samples 4m and 5i-8i are compared in the range 120-200 cm<sup>-1</sup> (range II) in Figure 3. The vibration at 164 cm<sup>-1</sup> for sample 8i can be interpreted as the symmetric vibration of  $A_{1g}(Br_6)$ . For samples with mixed inner ligands, due to the presence of isomers and nonequivalence of Br atoms co-ordinated to Re atoms with different environments of  $\mu_3$ -ligands, the positions of vibrations of similar nature differ, leading to a significant broadening of the bands and change in their shape (in fact, the appearance of new bands). The vibration at 138 cm<sup>-1</sup> for 8i can be interpreted as asymmetric but also involving terminal bromine atoms (see Figure 3). Displacement of atoms in the 8i cluster during  $A_{1g}(Br_6)$  and  $E_g(Br_6)$  modes are shown schematically in Figures 3b and 3c, respectively.

Symmetry **2023**, 15, 1791 7 of 12

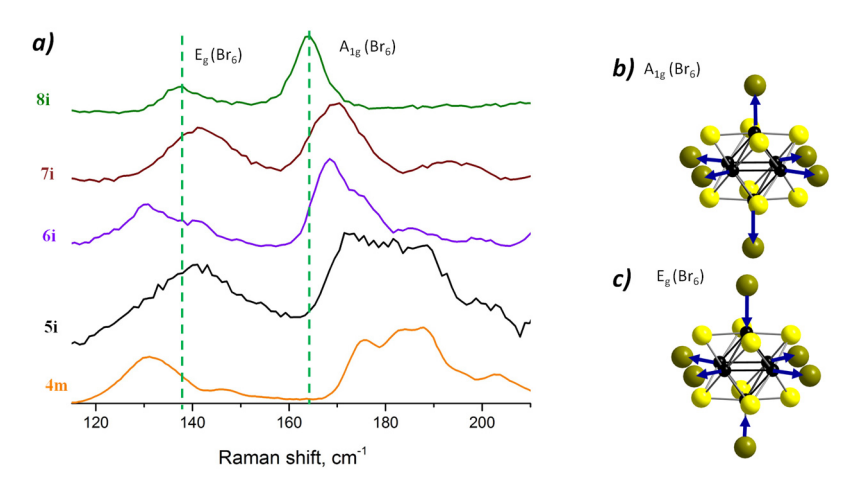


**Figure 3.** Raman spectra **4m**, and ionic **5i–8i** in the region **II** (a). Vertical dotted lines are drawn from the **8i** peaks. On the right, vibrations  $A_{1g}(Br_6)$  (b) and  $E_g$  (Br<sub>6</sub>) (c), in which Br atoms are involved, are schematically shown.

When sequentially considering the spectra of samples with mixed inner ligands in the cluster core, it can be seen that for 7i, a shift to higher frequencies is observed, while for 5i and 4m, a split of the peak into two is observed, with the opposite shift relative to the peak for 8i. Band shifts to the higher wavenumbers can be noted, however, a linear shift is observed only for the calculated spectra (Figure S5). In the region of ~60 cm<sup>-1</sup> (range III), corresponding to bending vibrations involving terminal bromide ligands, new bands also appear during replacement in the cluster core (Figure 1).

A comparison of Raman spectra of molecular 4m with a series of polymeric 5p-8p cluster compounds is shown in Figure 4. The change of the binding type of cluster cores with the formation of chains (5p) and 3D polymers (7p) and 8p leads to a significant change in the profiles of spectra.

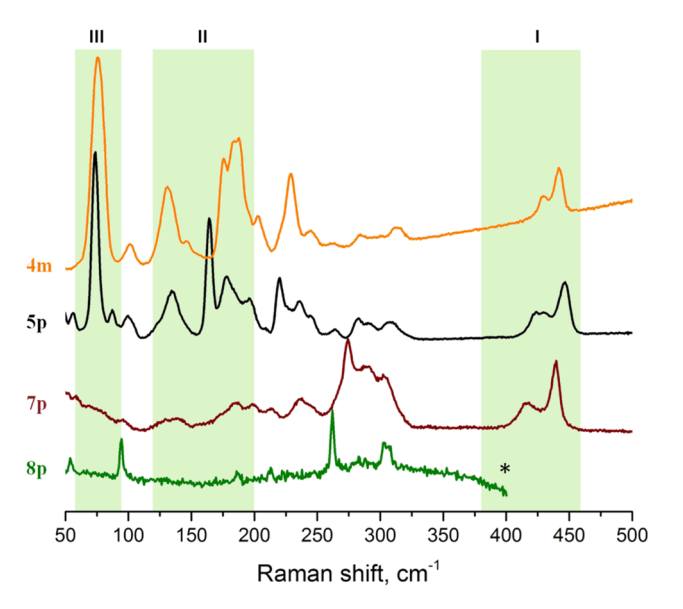


**Figure 4.** Raman spectra of polymer clusters **5p–8p** and molecular **4m**. Green rectangles indicate regions under detailed consideration, i.e., 380–460, 120–200, and 55–95 cm<sup>-1</sup> marked **I**, **II**, and **III**, respectively. \* Data not available due to sample luminescence.

A set of modes in the region of 60– $80~\rm cm^{-1}$  (region I), corresponding to the "rock" of the terminal bromide ligand, which was observed for all ionic and molecular clusters, is present in the case of polymeric clusters only for 5p with a chain structure. This vibration is blocked with an increase in the bonding, since the binding of the terminal bromine atoms

Symmetry **2023**, 15, 1791 8 of 12

occurs, thus leading to a formation of  $\mu$ -Br bridges. There are various collective vibrations affecting the terminal Br atoms (analogues of the  $A_{1g}(Br_6)$  vibration in 8i) in the region of 170–200 cm<sup>-1</sup> (region II). With increasing connectivity of the clusters, the intensity of these vibrations decreases, which can be associated with a decrease in the number and diversity of terminal Br atoms. In the range of 400–450 cm<sup>-1</sup> (region I), a pair of vibrations is observed, which manifests itself in all clusters (except for 8p, for which the spectrum is poorly resolved due to luminescence); apparently, these are analogs of the  $T_{2g}$  and  $A_{1g}(S_8)$  vibrations for 8i. Shifts of these vibrations in this series are observed in the same direction as for ionic clusters, but not so uniformly.

## 3.2. Far IR Spectroscopy

The complete vibrational representation, for example, for cluster 8i with  $O_h$  symmetry can be represented as

$$\Gamma = 3A_{1g}(R) + A_{2g} + 3E_g(R) + 3F_{1g} + 4F_{2g}(R) + A_{2u} + E_u + 3F_{1u}(IR) + 3F_{2u}$$

(The activity of vibrations in IR and Raman spectroscopy is indicated in parentheses by IR and R, respectively). Thus, different selection rules in IR and Raman spectroscopy lead to the appearance of different modes in the spectra, which helps to refine the structural information.

For all compounds in the series, we have recorded IR spectra (Figure 5, and also see combined Raman and IR spectra in Figures S9–S16). Figure 5 shows the IR spectra of compounds 5i–8i and 4m. The spectrum of the 8i cluster with the  $\{Re_6S_8\}^{2+}$  core contains the least number of modes in this series. This is probably due to its high symmetry and the absence of isomers. When sulfur atoms are replaced by bromine in the cluster core, low-intensity bands appear in the spectra. However, three groups of major intense fluctuations remain. A significant vibration is in the region of 400–430 cm<sup>-1</sup>, and the position of the peak changes smoothly in the series: 5i (423 cm<sup>-1</sup>), 6i (418 cm<sup>-1</sup>), 7i (414 cm<sup>-1</sup>) and 8i (407 cm<sup>-1</sup>). These vibrations can be attributed to vibrations affecting the  $\mu_3$ -S, stretching vibrations Re–S. For the molecular complex 4m, the peak broadens and splits, which could be due to a large number of isomers.

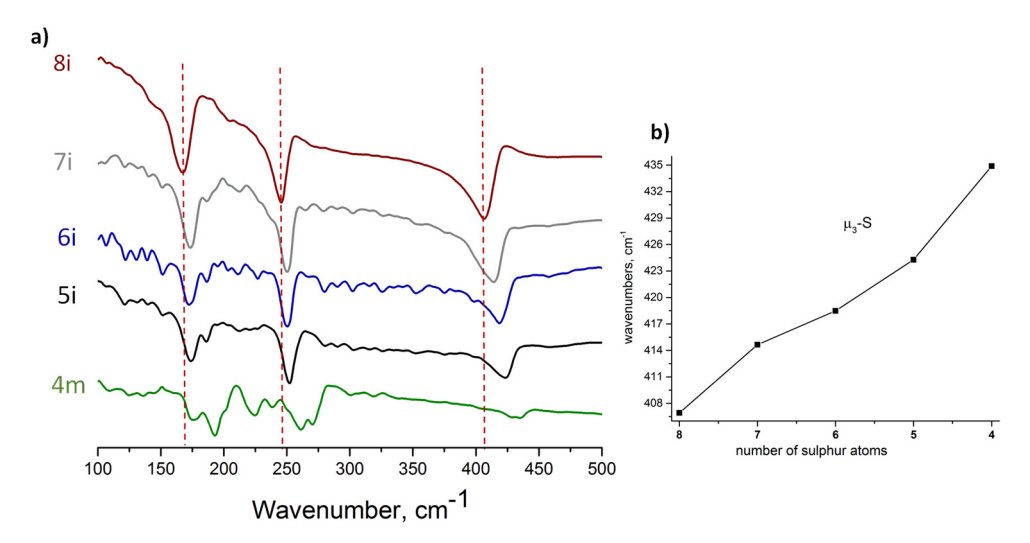


**Figure 5.** (a) Infrared spectra of 4m and 5i–8i; vertical dotted lines are drawn from the 8i peaks; (b) changing the position bands of the valence  $\mu_3$ -S vibrations.

The group of vibrations in the range of 242–252 cm<sup>-1</sup> can be attributed to the Re–Re [53] vibrations. It should be noted that for **6i** and **7i** the position of the peak is the same (250 cm<sup>-1</sup>, see Figure S8). Vibrations in the region of 170 cm<sup>-1</sup> are referred to as Re–Br stretching vibrations.

Symmetry **2023**, 15, 1791 9 of 12

The IR spectra of polymeric **5p–8p** compounds are shown in Figure 6. Three intense groups of bands at about 400, 270–290, and 170–19 cm<sup>-1</sup> corresponding to the Re–S, Re–Re, and Re–Br vibrations, respectively, can be distinguished. It is worth noting the splitting of the Re–S oscillations in **8p**, especially in comparison to **8i** (Figure 7). This is explained by the fact that in the polymer structure of **8p**, sulfur atoms are not equivalent, since some of them participate in the binding of the cluster fragments [ $\{Re_6S^i_6S^{i-a}_{2/2}\}S_{2/2}^{a-i}Br^{a-a}_{4/2}\}$  [49].

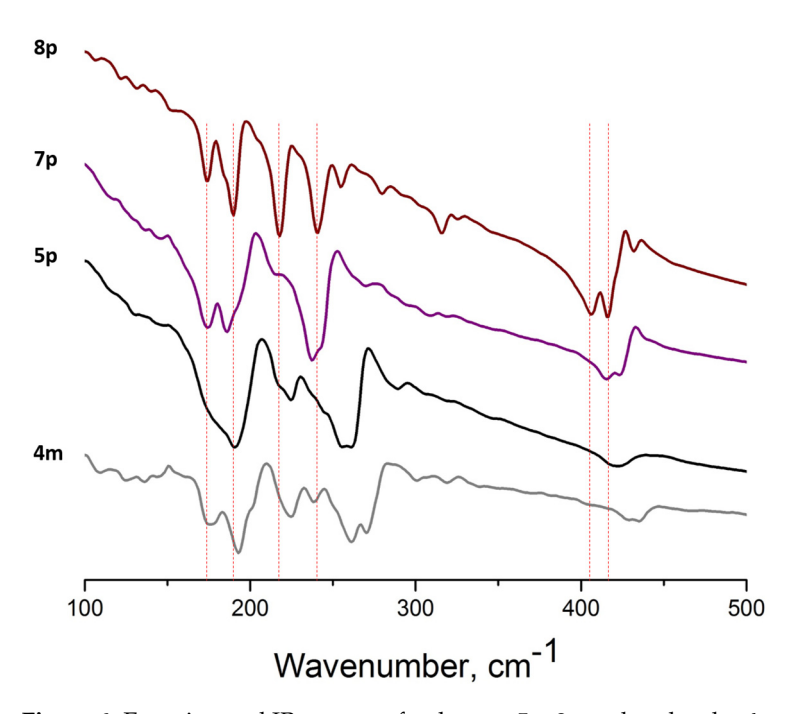
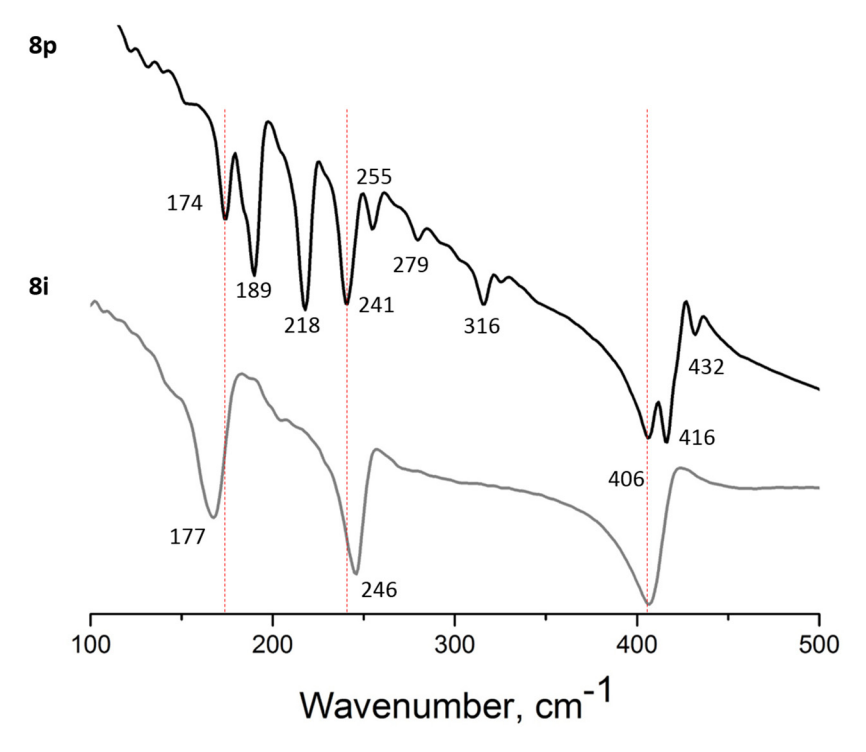


Figure 6. Experimental IR spectra of polymers 5p–8p and molecular 4m.



**Figure 7.** Comparison of experimental IR spectra of polymeric  $\mathbf{8p}$  and ionic  $\mathbf{8i}$  compounds with the same cluster core  $\{Re_6S_8\}$ .

Symmetry **2023**, 15, 1791 10 of 12

#### 4. Conclusions

A set of experimental and achieved by DFT calculations IR and Raman spectra for a number of octahedral cluster complexes with monotonically varying composition of the cluster core  $\{Re_6Q_{8-x}Br_x\}$  has been obtained. It is shown that the set of main characteristic bands  $(A_{1g}(S) T_{2g}(S), A_{1g}(Br), E_g(Br))$  is retained in both ionic and polymeric compounds. The observed vibration frequencies of these bands depend on the S/Br ratio in the cluster core. The difference in the connectivity in polymeric compounds leads to an increase in the number of bands in the spectra. The data obtained allow the identification of these cluster forms in solids and will be further useful for the identification of rhenium octahedral clusters in crystalline and, especially, in non-crystalline materials.

**Supplementary Materials:** The following supporting information can be downloaded at: https://www.mdpi.com/article/10.3390/sym15091791/s1, calculated Raman spectra of isomers **4m–8i**, combined Raman and IR spectra of **5p–8p** and **4m–8i**, and some other pieces of information are located in Supplementary Information.

**Author Contributions:** Conceptualization, N.G.N.; synthesis and characterization of polymeric and molecular compounds, S.S.Y.; synthesis and characterization of ionic compounds, A.Y.L.; IR spectroscopy, M.N.I.; Raman spectroscopy B.A.K.; DFT calculations, P.A.P.; writing—original draft preparation, A.Y.L.; supervision, V.E.F. All authors have read and agreed to the published version of the manuscript.

**Funding:** This work was carried out with the financial support of the Russian Science Foundation (project RSF no. 22-23-00626, agreement dated 29 December 2021, https://rscf.ru/project/22-23-00626/).

**Data Availability Statement:** The raw data presented in this study are available on request from the corresponding author.

**Acknowledgments:** The authors thank the Centre of Collective Usage of the Nikolaev Institute of Inorganic Chemistry SB RAS for experimental Raman and IR data collection (the Ministry of Science and Higher Education of the Russian Federation, N 121031700321-3, accessed on 1 December 2022).

Conflicts of Interest: The authors declare no conflict of interest.

### References

- 1. Gray, T.G. Hexanuclear and higher nuclearity clusters of the Groups 4–7 metals with stabilizing  $\pi$ -donor ligands. *Coord. Chem. Rev.* **2003**, 243, 213–235. [CrossRef]
- 2. Prokopuk, N.; Shriver, D.F. The Octahedral M<sub>6</sub>Y<sub>8</sub> And M<sub>6</sub>Y<sub>12</sub> Clusters of Group 4 and 5 Transition Metals. *Adv. Inorg. Chem.* **1998**, *46*, 1–49. [CrossRef]
- 3. Saito, T. Rhenium sulfide cluster chemistry. J. Chem. Soc. Dalton. Trans. 1999, 97–106. [CrossRef]
- 4. Gabriel, J.-C.P.; Boubekeur, K.; Uriel, S.; Batail, P. Chemistry of Hexanuclear Rhenium Chalcohalide Clusters. *Chem. Rev.* **2001**, 101, 2037–2066. [CrossRef]
- 5. Perrin, A.; Perrin, C. Low-Dimensional Frameworks in Solid State Chemistry of Mo<sub>6</sub> and Re<sub>6</sub> Cluster Chalcohalides. *Eur. J. Inorg. Chem.* **2011**, 2011, 3848–3856. [CrossRef]
- 6. Gray, T.G.; Rudzinski, C.M.; Meyer, E.E.; Holm, R.H.; Nocera, D.G. Spectroscopic and Photophysical Properties of Hexanuclear Rhenium(III) Chalcogenide Clusters. *J. Am. Chem. Soc.* **2003**, 125, 4755–4770. [CrossRef] [PubMed]
- 7. Kitamura, N.; Ueda, Y.; Ishizaka, S.; Yamada, K.; Aniya, M.; Sasaki, Y. Temperature Dependent Emission of Hexarhenium(III) Clusters [Re<sub>6</sub>( $\mu_3$ -S)<sub>8</sub>X<sub>6</sub>]<sup>4-</sup> (X = Cl<sup>-</sup>, Br<sup>-</sup>, and I<sup>-</sup>): Analysis by Four Excited Triplet-State Sublevels. *Inorg. Chem.* **2005**, 44, 6308–6313. [CrossRef]
- 8. Wilson, W.B.; Stark, K.; Johnson, D.B.; Ren, Y.; Ishida, H.; Cedeño, D.L.; Szczepura, L.F. Photophysical Properties of a Series of Rhenium Selenide Cluster Complexes Containing Nitrogen-Donor Ligands. Eur. J. Inorg. Chem. 2014, 2014, 2254–2261. [CrossRef]
- 9. Efremova, O.A.; Brylev, K.A.; Kozlova, O.; White, M.S.; Shestopalov, M.A.; Kitamura, N.; Mironov, Y.V.; Bauer, S.; Sutherland, A.J. Polymerisable octahedral rhenium cluster complexes as precursors for photo/electroluminescent polymers. *J. Mater. Chem. C* **2014**, *2*, 8630–8638. [CrossRef]
- 10. Ryzhikov, M.R.; Gayfulin, Y.M.; Ulantikov, A.A.; Arentov, D.O.; Kozlova, S.G.; Mironov, Y.V. Evolution of the Electronic Structure of the trans-[Re<sub>6</sub>S<sub>8</sub>bipy<sub>4</sub>Cl<sub>2</sub>] Octahedral Rhenium Cluster during Reduction. *Molecules* **2023**, *28*, 3658. [CrossRef]
- 11. Tarasenko, M.S.; Naumov, N.G.; Virovets, A.V.; Naumov, D.Y.; Kuratieva, N.V.; Mironov, Y.V.; Ikorskii, V.N.; Fedorov, V.E. New coordination polymers based on paramagnetic cluster anions  $[Re_6Se_8(CN)_6]^{3-}$  and rare earth cations: The synthesis and structure of  $[\{Ln(H_2O)_3)\}\{Re_6Se_8(CN)_6\}]\cdot 3.5H_2O$ . *J. Struct. Chem.* **2005**, *46*, S137–S144. [CrossRef]

Symmetry **2023**, 15, 1791 11 of 12

12. Echeverría, C.; Becerra, A.; Nuñez-Villena, F.; Muñoz-Castro, A.; Stehberg, J.; Zheng, Z.; Arratia-Perez, R.; Simon, F.; Ramírez-Tagle, R. The paramagnetic and luminescent [Re<sub>6</sub>Se<sub>8</sub>I<sub>6</sub>]<sup>3-</sup> cluster. Its potential use as an antitumoral and biomarker agent. *New J. Chem.* **2012**, *36*, 927–932. [CrossRef]

- 13. Ly, G.T.; Choi, J.; Kim, Y.; Kim, S.; Yang, S.-H.; Kim, S.-J. One-dimensional lead iodide hybrid stabilized by inorganic hexarhenium cluster cations as a new broad-band emitter. *RSC Adv.* **2021**, *11*, 24580–24587. [CrossRef] [PubMed]
- 14. Zhong, X.; Lee, K.; Choi, B.; Meggiolaro, D.; Liu, F.; Nuckolls, C.; Pasupathy, A.; De Angelis, F.; Batail, P.; Roy, X.; et al. Superatomic Two-Dimensional Semiconductor. *Nano Lett.* **2018**, *18*, 1483–1488. [CrossRef] [PubMed]
- 15. Roy, L.E.; Hughbanks, T. Electronic Transitions in  $[Re_6S_8X_6]^{4-}$  (X = Cl, Br, I): Results from Time-Dependent Density Functional Theory and Solid-State Calculations. *Inorg. Chem.* **2006**, *45*, 8273–8282. [CrossRef] [PubMed]
- 16. Telford, E.J.; Russell, J.C.; Swann, J.R.; Fowler, B.; Wang, X.; Lee, K.; Zangiabadi, A.; Watanabe, K.; Taniguchi, T.; Nuckolls, C.; et al. Doping-Induced Superconductivity in the van der Waals Superatomic Crystal Re<sub>6</sub>Se<sub>8</sub>Cl<sub>2</sub>. *Nano Lett.* **2020**, 20, 1718–1724. [CrossRef]
- 17. Kirakci, K.; Shestopalov, M.A.; Lang, K. Recent developments on luminescent octahedral transition metal cluster complexes towards biological applications. *Coord. Chem. Rev.* **2023**, *481*, 215048. [CrossRef]
- 18. Stass, D.V.; Vorotnikova, N.A.; Shestopalov, M.A. Direct observation of x-ray excited optical luminescence from a Re<sup>6</sup> metal cluster in true aqueous solution: The missing link between material characterization and in vivo applications. *J. Appl. Phys.* **2021**, 129, 183102. [CrossRef]
- 19. Krasilnikova, A.A.; Solovieva, A.O.; Ivanov, A.A.; Trifonova, K.E.; Pozmogova, T.N.; Tsygankova, A.R.; Smolentsev, A.I.; Kretov, E.I.; Sergeevichev, D.S.; Shestopalov, M.A.; et al. Comprehensive study of hexarhenium cluster complex Na<sub>4</sub>[{Re<sub>6</sub>Te<sub>8</sub>}(CN)<sub>6</sub>]—In terms of a new promising luminescent and X-ray contrast agent. *Nanomed. NBM* **2017**, *13*, 755–763. [CrossRef]
- Molard, Y.; Dorson, F.; Brylev, K.A.; Shestopalov, M.A.; Le Gal, Y.; Cordier, S.; Mironov, Y.V.; Kitamura, N.; Perrin, C. Red-NIR Luminescent Hybrid Poly(methyl methacrylate) Containing Covalently Linked Octahedral Rhenium Metallic Clusters. *Chem. Eur. J.* 2010, 16, 5613–5619. [CrossRef]
- 21. Amela-Cortes, M.; Cordier, S.; Naumov, N.G.; Mériadec, C.; Artzner, F.; Molard, Y. Hexacyano octahedral metallic clusters as versatile building blocks in the design of extended polymeric framework and clustomesogens. *J. Mater. Chem. C* **2014**, 2, 9813–9823. [CrossRef]
- 22. Molard, Y. Clustomesogens: Liquid Crystalline Hybrid Nanomaterials Containing Functional Metal Nanoclusters. *Acc. Chem. Res.* **2016**, *49*, 1514–1523. [CrossRef]
- 23. Suh, M.-J.; Vien, V.; Huh, S.; Kim, Y.; Kim, S.-J. Mesolamellar Phases Containing [ $Re_6Q_8(CN)_6$ ]<sup>4-</sup> (Q = Te, Se, S) Cluster Anions. *Eur. J. Inorg. Chem.* **2008**, 2008, 686–692. [CrossRef]
- 24. Kubeil, M.; Stephan, H.; Pietzsch, H.-J.; Geipel, G.; Appelhans, D.; Voit, B.; Hoffmann, J.; Brutschy, B.; Mironov, Y.V.; Brylev, K.A.; et al. Sugar-Decorated Dendritic Nanocarriers: Encapsulation and Release of the Octahedral Rhenium Cluster Complex [Re<sub>6</sub>S<sub>8</sub>(OH)<sub>6</sub>]<sup>4-</sup>. *Chem. Asian J.* **2010**, *5*, 2507–2514. [CrossRef]
- 25. Nguyen, N.T.K.; Lebastard, C.; Wilmet, M.; Dumait, N.; Renaud, A.; Cordier, S.; Ohashi, N.; Uchikoshi, T.; Grasset, F. A review on functional nanoarchitectonics nanocomposites based on octahedral metal atom clusters (Nb<sub>6</sub>, Mo<sub>6</sub>, Ta<sub>6</sub>, W<sub>6</sub>, Re<sub>6</sub>): Inorganic 0D and 2D powders and films. *Sci. Technol. Adv. Mater.* **2022**, *23*, 547–578. [CrossRef] [PubMed]
- 26. He, S.; Evans, A.M.; Meirzadeh, E.; Han, S.Y.; Russell, J.C.; Wiscons, R.A.; Bartholomew, A.K.; Reed, D.A.; Zangiabadi, A.; Steigerwald, M.L.; et al. Site-Selective Surface Modification of 2D Superatomic Re<sub>6</sub>Se<sub>8</sub>. *J. Am. Chem. Soc.* **2022**, *144*, 74–79. [CrossRef] [PubMed]
- 27. Cordier, S.; Fabre, B.; Molard, Y.; Fadjie-Djomkam, A.B.; Tournerie, N.; Ledneva, A.; Naumov, N.G.; Moreac, A.; Turban, P.; Tricot, S.; et al. Covalent Anchoring of Re<sub>6</sub>Se<sub>8</sub><sup>i</sup> Cluster Cores Mono layers on Modified n- and p-Type Si(111) Surfaces: Effect of Coverage on Electronic Properties. *J. Phys. Chem. C* **2010**, *114*, 18622–18633. [CrossRef]
- 28. Shores, M.P.; Beauvais, L.G.; Long, J.R. Cluster-Expanded Prussian Blue Analogues. J. Am. Chem. Soc 1999, 121, 775–779. [CrossRef]
- 29. Beauvais, L.G.; Shores, M.P.; Long, J.R. Cyano-Bridged Re<sub>6</sub>Q<sub>8</sub> (Q = S, Se) Cluster-Metal Framework Solids: A New Class of Porous Materials. *Chem. Mater.* **1998**, *10*, 3783–3786. [CrossRef]
- 30. Fedorov, V.E.; Naumov, N.G.; Mironov, Y.V.; Virovets, A.V.; Artemkina, S.B.; Efremova, O.A.; Peak, U.-H. Inorganic coordination polymers based on chalcocyanyde cluster complexes. *J. Struct. Chem.* **2002**, *43*, 669–684. [CrossRef]
- Cordier, S.; Molard, Y.; Brylev, K.A.; Mironov, Y.V.; Grasset, F.; Fabre, B.; Naumov, N.G. Advances in the Engineering of Near Infrared Emitting Liquid Crystals and Copolymers, Extended Porous Frameworks, Theranostic Tools and Molecular Junctions Using Tailored Re<sub>6</sub> Cluster Building Blocks. J. Clust. Sci. 2015, 26, 53–81. [CrossRef]
- 32. Cheplakova, A.M.; Kovalenko, K.A.; Shestopalov, M.A.; Brylev, K.A.; Fedin, V.P. Rhenium octahedral clusters in mesoporous MIL-101: Luminescence and sorption properties. *Russ. Chem. Bull.* **2014**, *63*, 1487–1492. [CrossRef]
- 33. Ivanov, A.A.; Falaise, C.; Shmakova, A.A.; Leclerc, N.; Cordier, S.; Molard, Y.; Mironov, Y.V.; Shestopalov, M.A.; Abramov, P.A.; Sokolov, M.N.; et al. Cyclodextrin-Assisted Hierarchical Aggregation of Dawson-type Polyoxometalate in the Presence of {Re<sub>6</sub>Se<sub>8</sub>} Based Clusters. *Inorg. Chem.* **2020**, *59*, 11396–11406. [CrossRef] [PubMed]
- 34. Selby, H.D.; Roland, B.K.; Zheng, Z. Ligand-Bridged Oligomeric and Supramolecular Arrays of the Hexanuclear Rhenium Selenide Clusters—Exploratory Synthesis, Structural Characterization, and Property Investigation. *Acc. Chem. Res.* 2003, 36, 933–944. [CrossRef] [PubMed]

Symmetry **2023**, *15*, *1791* 

35. Selby, H.D.; Zheng, Z. New directions of cluster chemistry—The story of the  $[Re_6(\mu_3-Se)_8]^{2+}$  clusters. *Comments Inorg. Chem.* **2005**, 26, 75–102. [CrossRef]

- 36. Xie, J.; Wang, L.; Anderson, J.S. Heavy chalcogenide-transition metal clusters as coordination polymer nodes. *Chem. Sci.* **2020**, 11, 8350–8372. [CrossRef] [PubMed]
- 37. Litvinova, Y.M.; Gayfulin, Y.M.; Kovalenko, K.A.; Samsonenko, D.G.; van Leusen, J.; Korolkov, I.V.; Fedin, V.P.; Mironov, Y.V. Multifunctional Metal–Organic Frameworks Based on Redox-Active Rhenium Octahedral Clusters. *Inorg. Chem.* **2018**, *57*, 2072–2084. [CrossRef]
- 38. te Velde, G.; Bickelhaupt, F.M.; Baerends, E.J.; Fonseca Guerra, C.; van Gisbergen, S.J.A.; Snijders, J.G.; Ziegler, T. Chemistry with ADF. J. Comput. Chem. 2001, 22, 931–967. [CrossRef]
- 39. Van Lenthe, E.; Baerends, E.J. Optimized Slater-type basis sets for the elements 1–118. *J. Comput. Chem.* **2003**, 24, 1142–1156. [CrossRef]
- 40. Perdew, J.P. Density-functional approximation for the correlation energy of the inhomogeneous electron gas. *Phys. Rev. B* **1986**, 33, 8822–8824. [CrossRef]
- 41. van Lenthe, E.; Ehlers, A.; Baerends, E.-J. Geometry optimizations in the zero order regular approximation for relativistic effects. *J. Chem. Phys.* **1999**, *110*, 8943–8953. [CrossRef]
- 42. Slougui, A.; Perrin, A.; Sergent, M. Structure of potassium hexarhenium nonabromide pentasulfide: KRe<sub>6</sub>S<sub>5</sub>Br<sub>9</sub>. *Acta Cryst. Sect. C* **1992**, *48*, 1917–1920. [CrossRef]
- 43. Slougui, A.; Ferron, S.; Perrin, A.; Sergent, M. Anionic charge effects on the crystal structures of Re6 octahedral cluster based compounds: The structure of the cubic bromide K<sub>2</sub>Re<sub>6</sub>S<sub>6</sub>Br<sub>8</sub>. *J. Clust. Sci.* **1997**, *8*, 349–359. [CrossRef]
- 44. Solodovnikov, S.F.; Yarovoi, S.S.; Mironov, Y.V.; Vironets, A.V.; Fedorov, V.E. Unusual Disordering of Potassium Ions in the Structures of Cluster Rhenium Thiohalides K<sub>3</sub>[Re<sub>6</sub>S<sub>7</sub>Br<sub>7</sub>] and K<sub>4</sub>[Re<sub>6</sub>S<sub>8</sub>Cl<sub>6</sub>]. *J. Struct. Chem.* **2004**, *45*, 865–873. [CrossRef]
- 45. Pilet, G.; Cordier, S.; Perrin, C.; Perrin, A. Single-crystal structure of Cs<sub>2</sub>Re<sub>6</sub>S<sub>6</sub>Br<sub>8</sub> rhenium thiobromide with acentric Re6 octahedral cluster units. *J. Struct. Chem.* **2007**, *48*, 680–689. [CrossRef]
- 46. Leduc, L.; Perrin, A.; Sergent, M.; Le Traon, F.; Pilet, J.C.; Le Traon, A. Rhenium octahedral clusters: Characterization of Re<sub>6</sub>Se<sub>4</sub>Cl<sub>10</sub> and the parent compound Re<sub>6</sub>Se<sub>4</sub>Br<sub>10</sub>. *Mater. Lett.* **1985**, *3*, 209–215. [CrossRef]
- 47. Perricone, A.; Slougui, A.; Perrin, A. Rhenium octahedral clusters: The systems Re-S-Br and M-Re-S-Br (M = Na, K, RB, Cs). *Solid State Sci.* **1999**, *1*, 657–666. [CrossRef]
- Perrin, A.; Leduc, L.; Sergent, M. Halogen bridged Re<sub>8</sub>L<sub>8</sub> units in octahedral cluster rhenium chalcohalides. Eur. J. Solid State Inorg. Chem 1991, 28, 919–931.
- 49. Fischer, C.; Alonso-Vante, N.; Fiechter, S.; Tributsch, H.; Reck, G.; Schulz, W. Structure and photoelectrochemical properties of semiconducting rhenium cluster chalcogenides: Re<sub>6</sub>X<sub>8</sub>Br<sub>2</sub> (X = S, Se). *J. Alloys Compd.* **1992**, *178*, 305–314. [CrossRef]
- 50. Schäfer, H.; Schnering, H.G.v. Metall-Metall-Bindungen bei niederen Halogeniden, Oxyden und Oxydhalogeniden schwerer Übergangsmetalle Thermochemische und strukturelle Prinzipien. *Angew. Chem.* **1964**, *76*, 833–849. [CrossRef]
- 51. Yoshimura, T.; Matsuda, A.; Ito, Y.; Ishizaka, S.; Shinoda, S.; Tsukube, H.; Kitamura, N.; Shinohara, A. Photoluminescent Properties of Chalcobromide—capped Octahedral Hexarhenium(III) Complexes [{Re<sub>6</sub>Q<sub>8-n</sub>Br<sub>n</sub>}Br<sub>6</sub>]<sup>n-4</sup> (Q = Se, n = 1–3; Q = S, n = 1, 2). *Inorg. Chem.* **2010**, *49*, 3473–3481. [CrossRef]
- 52. Yarovoi, S.S.; Solodovnikov, S.F.; Tkachev, S.V.; Mironov, Y.V.; Fedorov, V.E. Synthesis, structure, and 77Se NMR study of the (PPh<sub>4</sub>)<sub>2</sub>[Re<sub>6</sub>Se<sub>6</sub>Br<sub>8</sub>] complex. *Russ. Chem. Bull.* **2003**, 52, 68–72. [CrossRef]
- 53. Griffith, W.P.; Kiernan, P.M.; O'Hare, B.P.; Brégeault, J.M. Vibrational spectra of the  $[Re(CN)_7]^{4-}$ ,  $[V(CN)_7]^{4-}$ ,  $[Nb(CN)_6]^{4-}$ ,  $[Re_4S_4(CN)_{12}]^{4-}$  and  $[Re_4S_4(CN)_{12}]^{4-}$  ions. *J. Mol. Struct.* **1978**, 46, 307–317. [CrossRef]

**Disclaimer/Publisher's Note:** The statements, opinions and data contained in all publications are solely those of the individual author(s) and contributor(s) and not of MDPI and/or the editor(s). MDPI and/or the editor(s) disclaim responsibility for any injury to people or property resulting from any ideas, methods, instructions or products referred to in the content.